Mon. Not. R. Astron. Soc. **377,** 1579–1587 (2007) doi:10.1111/j.1365-2966.2007.11719.x

Heavy calcium in CP stars⋆

C. R. Cowley,[1]† S. Hubrig,[2]† F. Castelli,[3]† J. F. González[4]† and B. Wolff[5]†

[1]*Department of Astronomy, University of Michigan, Ann Arbor, MI 48109-1042, USA*
[2]*European Southern Observatory, Casilla 19001, Santiago 19, Chile*
[3]*INAF-Osservatorio Astronomico di Trieste, Via G. B. Tiepolo 11, 34131 Trieste, Italy*
[4]*Complejo Astronómico El Leoncito, Casilla 467, 5400 San Juan, Argentina*
[5]*European Southern Observatory, Karl-Schwarzschild-Str. 2, 85748 Garching, Germany*

Accepted 2007 March 8. Received 2007 February 22; in original form 2007 January 16

ABSTRACT

Large wavelength shifts of infrared triplet lines of Ca II have been observed in the spectra of HgMn and magnetic Ap stars. They have been attributed to the heavy calcium isotopes, including ^{48}Ca. One member of the triplet, λ8542, had been either unavailable, or of poor quality in earlier spectra. The present material shows conclusively that the stellar λ8542 shifts are consistent with an interpretation in terms of ^{48}Ca. We find no relation between isotopic shifts of the Ca II triplet lines, and those of Hg II λ3984. There is a marginal indication that the shifts are *anticorrelated* with the surface field strengths of the magnetic stars. We see sparse evidence for ^{48}Ca in other chemically peculiar stars, for example, Am stars, metal-poor stars or chemically peculiar red giants. However, the sample is still very small, and the wavelengths of all three triplet lines, including those in the Sun, show slight positive shifts with respect to terrestrial positions.

Some profiles of the Ca II infrared triplet in the magnetic stars show extensive wings beyond a well-defined core. We can obtain reasonable fits to these profiles using a stratified calcium abundance similar to that used by previous workers. There is no indication that either the stratification or the Zeeman effect significantly disturbs the measurement of isotope shifts.

Key words: stars: atmospheres – stars: chemically peculiar – stars: magnetic fields.

1 INTRODUCTION

Calcium is the only chemical element with two stable, doubly magic isotopes. The two nuclides,^{40}Ca and ^{48}Ca, are the lightest and heaviest of calcium's six stable isotopes. Clayton (2003) describes the cosmochemistry of calcium with an emphasis on the unusual properties of its isotopes.

The infrared triplet of Ca II arises from 3d levels, which fall between the ground 4s and 4p terms giving rise to the H and K resonance lines at λλ3933 and 3968. The lines of the triplet have wavelengths 8498.02, 8542.09 and 8662.14 Å. The precise values differ slightly, depending on the source. We adopt here the values given in the NIST online Handbook (Sansonetti & Martin 2003).

Differences less than 0.01 Å occur between these values and those obtained from subtracting energy levels in Sugar & Corliss (1985). They are unimportant in the present context.

Laboratory work on the infrared triplet was described by Nörtershäuser et al. (1998). They report shifts of +0.21, +0.20 and +0.20 Å for λλ8662, 8542 and 8498, respectively, for ^{48}Ca II relative to ^{40}Ca II. Such displacements are easily measured on high-resolution astronomical spectra. The shifts for the infrared triplet are much larger than corresponding shifts for the 4s–4p resonance lines (≈0.01 Å, Mårtensson-Pendrill et al. 1992). The large shifts are due to the high angular momentum and relatively concentrated charge density of the 3d electron of the lower term of the triplet.

The wavelengths of the triplet for isotopically pure calcium are given in Table 1 from Nörtershäuser et al. (see their table 2) but converted to angstrom units. Note that these authors give shifts only of λ8542 for ^{46}Ca. They investigated hyperfine structure for the odd-*A* isotope, ^{43}Ca, but the widths are relatively small, and are ignored here.

Castelli & Hubrig (2004) first announced detection of ^{48}Ca in several HgMn (CP3) stars. Cowley & Hubrig (2005) subsequently found a similar effect in magnetic Ap (CP2) stars. The shifts appear to vary from those indicating nearly pure ^{48}Ca to a virtual terrestrial mix (nearly pure ^{40}Ca). Most stars show some shifts indicating heavy Ca isotopes, as we will illustrate in the figures below. This is true for the Sun also, though the significance of this observation is yet unclear.

⋆Based on observations obtained at the European Southern Observatory, Paranal and La Silla, Chile [ESO programmes 076.D-0169(A) and 076.C-0172(A)].

†E-mail: cowley@umich.edu (CRC); shubrig@eso.org (SH); castelli@ts.astro.it (FC); fgonzalez@casleo.gov.ar (JFG); bwolff@eso.org (BW)

Table 1. Isotopic wavelengths of Ca II infrared triplet (Nörtershäuser et al. 1998).

Mass no.	Laboratory λ (Å)	Isotopic λ (Å)	Shift (Å)
42	8498.018	8498.074	0.057
42	8542.089	8542.146	0.057
42	8662.140	8662.199	0.059
43	8498.018	8498.101	0.083
43	8542.089	8542.173	0.084
43	8662.140	8662.226	0.087
44	8498.018	8498.126	0.108
44	8542.089	8542.198	0.109
44	8662.140	8662.252	0.113
46	8542.089	8542.247	0.158
48	8498.018	8498.218	0.200
48	8542.089	8542.291	0.202
48	8662.140	8662.347	0.208

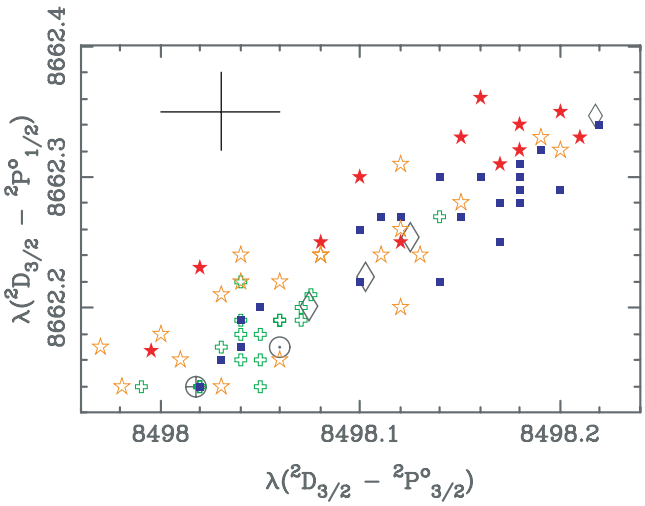

Figure 1. Wavelengths of Ca II λ8662 are correlated with those for λ8498. Filled squares are HgMn stars; filled and open stars are for roAp and noAp stars, respectively. Open crosses are for miscellaneous types. Solar wavelengths are indicated by the sun symbol. Diamonds indicate wavelengths for pure isotopes of mass 42, 43, 44 and 48, as given by Nörtershäuser et al. (1998). Wavelengths from the NIST web site are indicated by an Earth symbol (⊕); the terrestrial mix is 97 per cent ^{40}Ca. Error estimates are indicated in the upper left-hand portion of the figure.

2 OBSERVATIONS AND THEIR MEASUREMENT

The spectra used in this study have been obtained either with the UV-Visual Echelle Spectrograph (UVES) at UT2 of the VLT or with the FEROS echelle spectrograph on the 2.2-m telescope at La Silla. We used the UVES dichroic standard settings covering the spectral range from 3300 to 9300 Å. The slit width was set to 0.3 arcsec for the red arm, corresponding to a resolving power of $\lambda/\Delta\lambda \approx 110\,000$. For the blue arm, we used a slit width of 0.4 arcsec to achieve a resolving power of ≈80 000. In 2004 November, three new standard dichroic settings with a central wavelength at 760 nm (Dic#2 346 + 760, 390 + 760, 437 + 760) were implemented. This reconfiguration made it possible to measure the λ8542 line, which had previously been unavailable because of an order gap.

The UVES spectra were reduced by the UVES pipeline Data Reduction Software (version 2.5), which is an evolved version of the ECHELLE context of MIDAS. The signal-to-noise ratios (S/N) of the obtained spectra differ, but range from about 100 to 400.

The wavelength coverage for the FEROS spectra is from 3530 to 9220 Å, but often omitting the λ8542 region. The nominal resolving power is 48 000, with an S/N of ca. 150–400. Basic steps of spectroscopic reduction (bias subtraction, division by a normalized flat field, extraction of a 1D spectrum and wavelength calibration) were based on IRAF.

The spectra were mildly Fourier filtered before the wavelengths were measured at Michigan. For a few stars, the wavelength positions were also determined by comparing the observed spectra with synthetic spectra. Table A1 gives measurements for all of the Ca II lines used in this paper.

3 THE STELLAR ISOTOPIC SHIFTS

Stellar wavelengths often differ slightly from their laboratory positions. For atomic spectra, this is only rarely due to isotopic effects. Far more often, two atomic lines blend together so that the measured position corresponds to a weighted mean of the two laboratory positions. Generally speaking, the stronger the line, the less likely its wavelength is to be perturbed. This is generally the situation with the Ca II lines in multiplet 2, known as the infrared triplet.

Wavelengths of symmetrical, unblended lines may be measured to an accuracy better than ±0.01 Å on high-resolution spectra of the kind discussed here. For asymmetrical features, such as those influenced by blending, differences up to 0.05 Å may occur for repeated measurements of the same feature; one measurement might reflect the centre of gravity of a feature, another the flux minimum.

The lines of the calcium infrared triplet are all formed on the wings of broad Paschen lines: P13, λ8665.02; P15, λ8545.39 and P16, λ8502.49. These hydrogen lines influence the depths of the nearby calcium features but any wavelength perturbations are below the level of accuracy considered here. Other nearby atomic lines are usually too weak to influence the measured wavelengths adopted for the calcium lines. Weak blends may be of some influence when combined with the effect of blending of isotopic profiles, or especially with Zeeman splitting.

We allow a liberal overall uncertainty in the measured positions, of about ±0.05 Å. Typical errors should be somewhat smaller than this, perhaps ±0.03 Å, as indicated in the figures.

In Fig. 1, all wavelengths listed in Table A1 for λλ8498 and 8662 are plotted. The number of objects previously studied for the ^{48}Ca anomaly are substantially increased over previous work (cf. Castelli & Hubrig 2004; Cowley & Hubrig 2005).

Fig. 1 shows that wavelength shifts for Ca II λ8498 and λ8662 are correlated with one another, as one would expect if they are isotopic. It is intriguing that most stars, *including the Sun*, have shifts that could be interpreted as having a larger admixture of heavier isotopes than in terrestrial materials.

Chmielewski (2000) noted these shifts for the solar lines, but the recent study of calcium in late-type stars (Mashonkina, Korn & Przybilla 2007) does not mention them. This may be due to the explicit inclusion of the isotopic wavelengths in the later work; unfortunately these authors do not give figures for the infrared triplet lines. Our own calculations including isotopic wavelengths produce a definite shift of the profiles to the red, though we still do not get satisfactory overall fits.

The discrepancy between the solar and laboratory wavelengths (0.03–0.04 Å) may arise from the fact that the laboratory

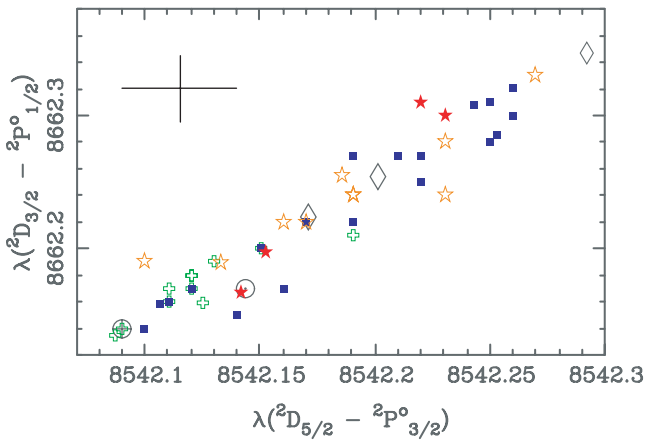

Figure 2. Measured wavelengths Ca II λ8662 versus those for λ8542. The symbols have the same meaning as in the previous figure.

measurements reflect wavelengths made on optically thin sources. Small contributions from the rare isotopes could then be missed. On the other hand, the solar features arise from lines that are optically thick. This would make the isotope shifts more evident. Thus, the small shifts are not necessarily due to isotopic anomalies.

Note that in a few instances, wavelengths *short* of the terrestrial position, λ8498.02, were measured. Similar results were occasionally obtained for the λ8542 and λ8662 lines. Some of these results are arguably due to measurement error. Other negative shifts occur for double-lined binaries (SB2), and are plausibly due to perturbations from the secondary spectrum.

The case for isotopic shifts is considerably strengthened by reliable measurements for the third line of the triplet, λ8542. Most of these became available only after the reconfiguration of the UVES spectrograph.

The results are shown in Fig. 2.

We can see that the wavelength displacements of all three of the Ca II infrared triplet are closely correlated.

4 RELATION TO ISOTOPIC ANOMALIES IN MERCURY

Several elements have isotopic anomalies in CP stars: He, Hg, Pt and Tl. We restrict consideration here to mercury, which has been investigated in a large number of CP3 (HgMn) stars. While both Hg and Pt are arguably present also in magnetic Ap or CP2 stars, their higher spectral line densities make conclusions about isotopic compositions difficult.

Bidelman (1962) reported the tentative identification of λ3984 in the spectrum of κ Cnc as Hg II. He supplied additional details of his work to Federer (1962), along with the interpretation that the mean wavelength variation from star to star of the Hg II feature indicated changes in the isotopic composition. Bidelman suggested that the λ3984 wavelength in χ Lup indicated nearly pure ^{204}Hg.

Fig. 3 gives no indication that the isotopic anomalies of calcium and mercury are correlated.

Preston (cf. Preston et al. 1971) and his coworkers noted a correlation of the isotopic mixture of mercury with stellar temperature. Interestingly, newer measurements of HgMn stars weaken the temperature–wavelength correlation discussed by previous workers. This may be seen from our Fig. 4. The closed circles are from Woolf & Lambert (1999), White et al. (1976) or Cowley & Aikman (1975). Neither Cowley and Aikman nor White et al. had stars with

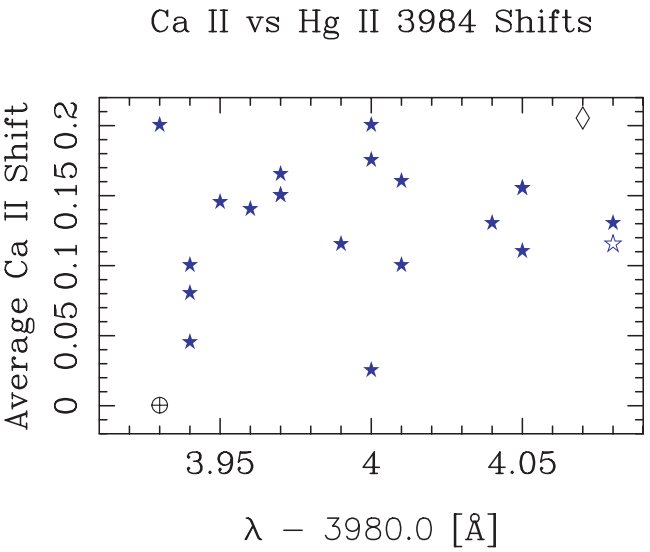

Figure 3. Average Ca II shifts (λ8498 and λ8662) versus Hg II λ3984 wavelength. There is no apparent correlation of calcium and mercury isotopic anomalies. Filled stars are HgMn stars. The open star is for Feige 86. Wavelengths for terrestrial calcium and mercury are indicated by an Earth symbol (⊕); the diamond is for pure ^{48}Ca and ^{204}Hg. We see no indication that isotopic anomalies are related.

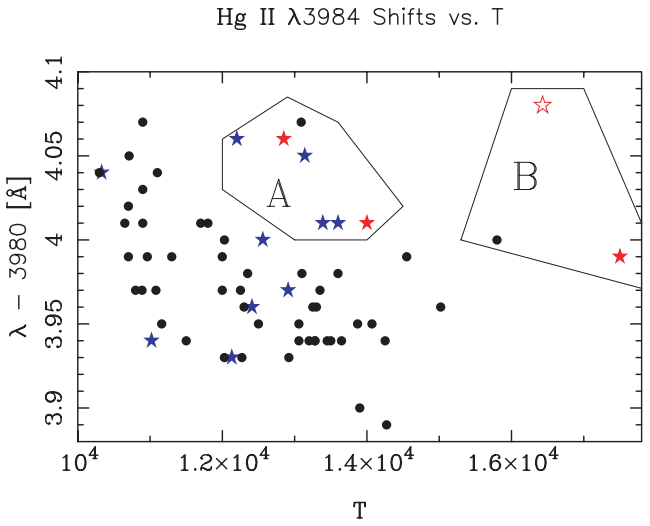

Figure 4. New measurements weaken the temperature correlation with isotopic anomalies in mercury. Measurements from previous workers are shown as filled circles. The star symbols are measurements from ESO spectra. The solid star in Region B is 3 Cen A, while the open star is Feige 86. See text for a discussion of the objects in Region A.

temperatures in the range 12 000–14 000 K with Hg II wavelengths ⩾3984.00 Å. But Woolf and Lambert's study already revealed at least two 'outliers', 46 Aql (12 900 K, 3984.073 Å), and HR 5998 (15,800 K, 3984.003 Å). To these we add several more. They fall in two regions denoted 'A' and 'B' in Fig. 4.

Several of the stars in Regions A and B are significantly different from the 'classical' HgMn stars, those studied in the 1970s. These include Fiege 86, the field horizontal branch star (cf. Bonifacio, Castelli & Hack 2001) and 3 Cen A (Castelli, Parthasarathy & Hack 1997) in Region B. The filled circle in Region B is for HR 5998. Its

Table 2. New data used for Fig. 4.

Name	HD number	Temperature	λ − 3980.0
CD −60 1951	65949	13 600	4.01
CD −60 1952	65950	12 910	3.97
κ^2 Vol	71066	12 200	4.06
HR 4487	101189	11 020	3.94
3CenA	120709	17 500	3.99
HR 6000	144667	12 850	4.06
HR 6870	168733	14 000	4.01
HR 7143	175640	12 130	3.93
Feige 86		16430	4.08

rather broad-lined spectrum resembles those of the classical HgMn stars.

The filled circle in Region A is 46 Dra, a 'marginal' Hg star (Dworetsky 1976). Region A also contains the unusual HR 6870 (Muthsam & Cowley 1984) and HR 6000 (Castelli & Hubrig 2006), which are significantly different from classical HgMn stars. The Hg II features are weak. We plot the point for HR 6000 high in Region A, as originally measured (by CRC), which would indicate nearly pure ^{204}Hg. Castelli and Hubrig's spectrum of HR 6000 shows that lighter isotopes are also present. A weighted mean, using the relative abundances they give would move the point for HR 6000 to the lower boundary of Region A. Another unusual object in Region A is HD 65949 (Cowley et al. 2006), whose Hg II line is very strong, while Mn II is relatively weak. The sharp-lined spectrum of κ^2 Vol is quite similar to that of 46 Aql. The remaining points in Region A belong to the double-lined binary υ^4Eri. One component resembles a classical HgMn star, while the other has Hg but relatively weak Mn.

Wavelength measurements for Hg II λ3984 were mostly taken from the references cited. Additional values from ESO spectra are listed in Table 2, along with temperatures from the literature, or based on photometry (Moon 1984).

5 Ca II SHIFTS: POSSIBLE TEMPERATURE CORRELATIONS

Fig. 5 shows average shifts for the two Ca II lines for which we have the most measurements, λλ8498 and 8662, plotted versus temperature. Filled squares are for the HgMn stars. The overall plot shows no indication of a correlation of the shifts with temperature. If one considers the magnetic and non-magnetic objects separately, there may be a weak correlation with temperature but in the opposite sense for the magnetic and non-magnetic stars.

Temperatures for the non-magnetic stars are from sources previously cited. Most of the temperatures for the magnetic stars are from Ryabchikova (2005a), or Hubrig, Nort & Mathys (2000). A temperature of 8100 K was used for HD 965, following Bord et al. (2003).

6 AN INVERSE CORRELATION WITH MAGNETIC FIELD STRENGTH?

Plots of the shifts for both λλ8498 and 8662 of the magnetic stars suggest that there could be an inverse correlation of the shifts of these two lines with surface magnetic field strength. This is illustrated for λ8498 in Fig. 6. A plot for λ8662 shows a quite similar trend, while one for λ8542, for which we have fewer measurement shows no correlation. It appears from the plots for λλ8498, and 8662 that the

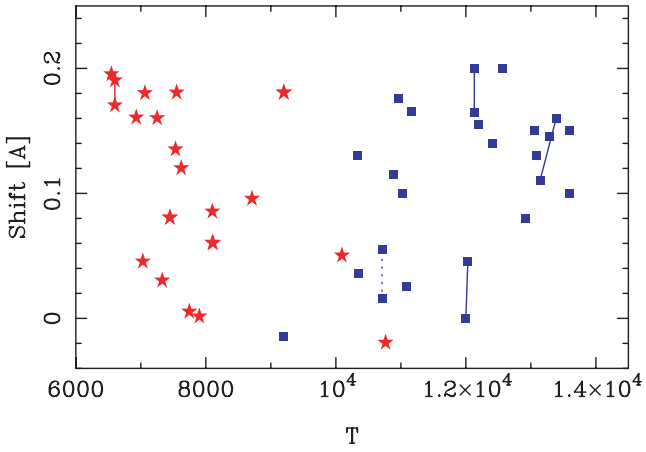

Figure 5. Average shifts of λλ8498 and 8662 for magnetic (stars) and HgMn (squares) stars are plotted against temperature. UVES and FEROS measures of HD 101065 (far left-hand side) and HR 7143 (upper right-hand side) are connected by a solid line. Measurements on the SB2 stars υ^4 Eri (far right-hand side) and 74 Aqr (lower right-hand side) are also connected. The dashed line connects measurements of the minimum (lower point) and centroid for the primary of χ Lup. See text for references to the Hg II wavelength measurements.

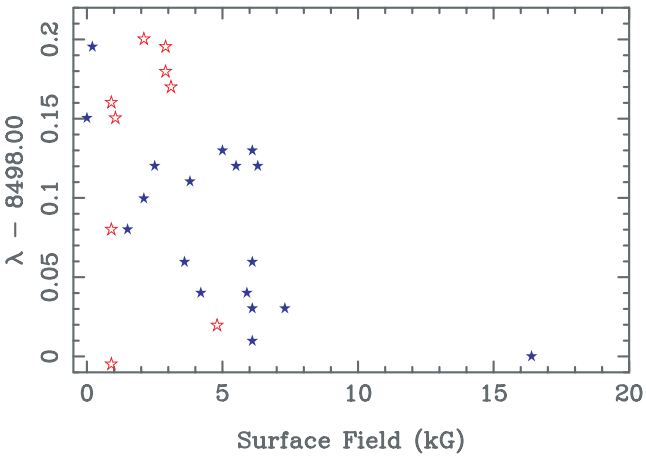

Figure 6. Wavelength shifts of λ8498 for roAp and noAp magnetic stars (open and solid symbols, respectively) are plotted versus the surface magnetic fields. The star with the large field is HD 47103.

inverse correlation, if real, is due to the non-oscillating magnetic stars (solid stars in Fig. 6).

We have measurements of one very strong-field star that definitely contradicts the overall trend of large shifts with weak fields. In HD 154708, Hubrig et al. (2005), measured a mean field of 24.5 kG. We measure displacements of +0.14, 0.26 and 0.29 for λλ8498, 8542 and 8662, respectively. Though the displacements are all positive, they are significantly different for one of the three lines. Possibly this difference is caused by, other effects than isotopic shifts – most likely, blending with highly displaced Zeeman components. We note with interest, however, the new classification of HD 154708 as a roAp star (Kurtz et al. 2006). This strengthens the suggestion that it is only the non-oscillating stars that obey the inverse correlation of field strengths and isotope shifts.

Clearly more measurements are necessary to establish this trend.

Magnetic field measurements are from Kurtz et al. (2006),

Hubrig et al. (2006), and measured on our spectra using the magnetically sensitive line Fe II λ6149 (cf. Mathys et al. 1997). For a few stars with unresolved λ6149 and only longitudinal field measurements available in the literature, we used the approximate relation $\langle B_S \rangle \approx 3\langle B_z \rangle$, assuming a dipole field. Error estimates for the fields vary from star to star, depending on the magnitude of the Zeeman splitting and the complexity of the profiles. Likely overall errors in the surface field values are of the order of a kilogauss.

7 PROFILES OF THE CA II TRIPLET IN THE MAGNETIC STARS

7.1 Approximate calculation of Zeeman profiles

We have attempted spectral synthesis of the Ca II lines in several stars. For those stars with wide Zeeman patterns, the spectra were synthesized using the assumption of a pure longitudinal or a pure transverse magnetic field. With these assumptions, the equations of radiative transfer for the Stokes parameters become diagonal (cf. del Toro Iniesta 2003), so that with the local thermodynamic equilibrium assumption one may use a standard code. For the longitudinal field assumption, separate calculations are made for the left- and right-hand sigma components, and the resultant flux *versus* wavelength files are averaged with equal weights. Similar calculations are made for both sigma and pi components for the transverse field assumption. We approximate the profiles for the general case by taking a weighted mean for longitudinal and transverse field orientations. This scheme is, of course, inferior to one using a full Stokes transfer, averaging over the specific intensity, provided the total surface field orientation is known. We believe it is a useful approximation in the absence of detailed knowledge of the field.

7.2 The stellar profiles

Even with the simplifications discussed above, spectral synthesis of the Ca II infrared triplet is fraught with difficulties. All three lines are formed in the wings of the Paschen lines, P13 (λ8662), P15 (λ8542) and P16 (λ8498). The VCS (Vidal, Cooper & Smith 1973) Stark profiles do not fit observed lines very well. This was noted by Frémat, Houziaux & Andrillat (1996).

The more recent tabulations of Stehlé & Hutcheon (1999), unfortunately, do not extend to large enough values of N_e (for P13–P16) to accommodate our models. We used Lemke's (1997) extended VCS tables, and leave the problem of fitting the Paschen lines for another study.

The presence of the Paschen lines, in addition to significant water–vapour absorption, makes it most difficult to normalize the observations to a continuum. This problem is exacerbated for echelle observations, where orders must be joined.

In the figures below, we have adjusted the observations slightly (up or down) to optimize the fits with the theory. This seems permissible, in view of normalization problems, and the approximate, working, model atmosphere used. We have not attempted to derive accurate abundances from the infrared triplet. The profile calculations were made to illustrate that in spite of difficulties with the continuum and the anomalous line shapes, *the cores can be reasonably fit, and therefore, the measured wavelengths are credible.*

All of the spectra illustrated in this section use an approximate ATLAS9 (Castelli & Kurucz 2003) model with a T_e of 7700 K, $\log(g) = 4.0$ and Ap-star abundances based on the results for γ Equ (Ryabchikova et al. 1997). The calculations assumed only one dominant calcium isotope.

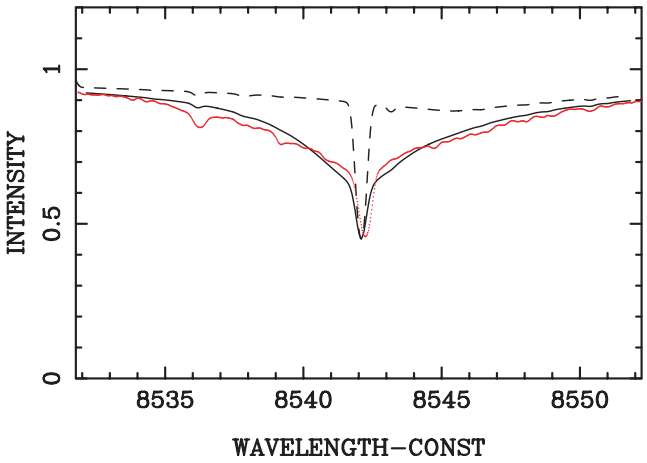

Figure 7. Ca II λ8542 in γ Equ. The observed spectrum is dotted. The slight P15 minimum is seen in the calculations at 8545.4 Å, but the influence of this line is small. Note the small displacement of the calculated minimum from the observed one, which we attribute to an admixture of ^{48}Ca. The solid curve employs the stratification described in the text, with Ca/Sum = 3×10^{-5} in the deepest layers. This is some 15 times the solar abundance of calcium. The dashed line results from no stratification and Ca/Sum = 4×10^{-9}. While the core is fitted, the failure in the wings is catastrophic.

7.3 Stratification

In the cooler magnetic stars, the lines of the infrared triplet appear to have very broad wings. This is illustrated in Fig. 7.

We have been able to account for the broad wings in γ Equ using a stratification essentially that of Ryabchikova et al. (2002, see also Ryabchikova 2005b). For convenience, we did use an analytical formula based on three positive parameters, a, b and d, to give the stratification profile. With $x = \log \tau_{5000}$, we multiply the abundance by a factor $g(x)$, where

$$g(x) = b + (1 - b)\left[\frac{1}{2}\sqrt{\left(\frac{\pi}{a}\right)} \pm \frac{1}{2}\mathrm{erf}(\sqrt{(a|x + d|^2)}\right] .$$

The negative sign applies for $x \leqslant -d$. This function is a smoothed step of height $1 - b$, located at depth $\log \tau_{5000} = -d$. The Gaussian 1/e width of the step is $1/\sqrt{a}$. We adjusted the parameters on a trial-and-error basis rather than attempt an inversion procedure, as discussed by Kochukhov et al. (2006). A recent preprint by Kochukhov (2007) describes a parameterized approach similar to ours. In the present work, we used stratification only for two stars (see Figs 7 and 8 below).

7.4 Moderate field strengths: γ Equ

The λ8542 line was fitted for γ Equ by a stratified model using $a = 6.7$, $b = 10^{-4}$ and $d = 1$. These parameters put an abundance jump of nearly 4 dex at $\log \tau_{5000} = -1$; the width of the jump is roughly one unit in $\log \tau_{5000}$. The stratification is quite similar to that already used by Ryabchikova et al. (2002). We can confirm that the same model accounts quite well for the stronger Ca II K-line profile.

The Zeeman components were not explicitly calculated, in view of the sharpness of the lines in this star; an enhanced microturbulence of 4 km s^{-1} was employed to simulate the magnetic effects. The results are shown in Fig. 7.

We synthesized several Ca I near λ6160, in γ Equ using our default model with and without stratification. We find that we can fit them with an abundance ratio of calcium to the sum of all elemental abundances, or Ca/Sum 6×10^{-6}, and $\xi_t = 4$ km s^{-1}, using our

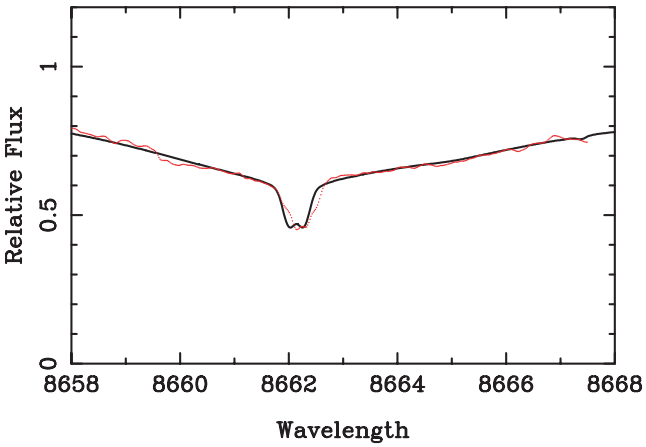

Figure 8. Ca II λ8662 in HD 51684. We see again the broad wings, suggestive of extreme damping. The measured wavelength shift for this line is 0.11 Å. The P13 core is at 8665 Å.

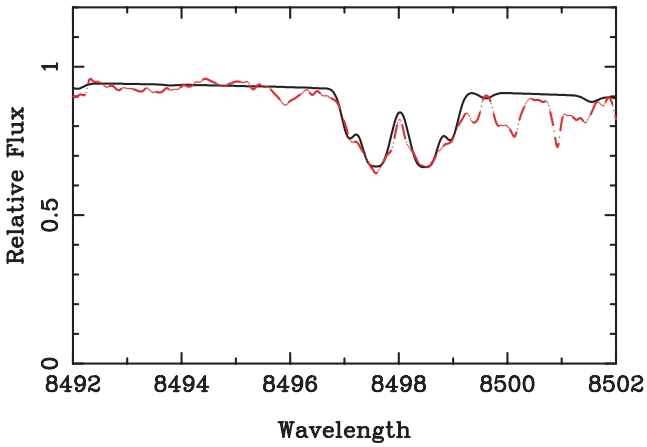

Figure 9. Ca II λ8498 in HD 47103 (17.5 kG). Wavelength measures of lines with doublet splitting such as that shown must be of the *maximum flux* between the two components. This calculation used a longitudinal to transverse field ratio of 2 to 3, and an abundance Ca/Sum of 6.5×10^{-8}. No stratification was assumed.

model. This is also near the value found in the work cited. For these relatively weak Ca I lines, the stratification was of minor importance.

7.5 The triplet at higher field strengths

For surface fields of 10 kG or more, the Zeeman patterns are obvious in stars with minimal rotational broadening. Components of the λ8498 line, the weakest of the three Ca II lines, split into a doublet structure. The remaining two lines resolve into triplets for sufficiently high fields. At our resolution, closely spaced Zeeman components are not seen individually.

HD 51684 has an surface field of 6.3 kG, according to our measurement of the splitting of the magnetically sensitive Fe II line, λ6149. However, for the λ8662 line, we got a somewhat better fit using 5 kG. We show a Zeeman synthesis of the λ8662 line in Fig. 8, where the components are marginally resolved. Our best fit (shown) assumed a 3 to 1 ratio of longitudinal to transverse fields. The stratification parameters were $a = 4.0$, $b = 0.001$ and $d = 1.0$. The figure was made with Ca/Sum $= 2 \times 10^{-4}$.

HD 47103 is one of our stars with the strongest fields. The λ8498 line shows a wide doublet structure (Fig. 9). The broad wings seen in the previous figures are not evident, and stratification was not used.

We determined a mean surface field of 16.4 kG from Fe II λ6149. However, the fit shown in Fig. 9 is slightly better if we use the surface field of 17.5 kG (cf. Babel, North & Queloz 1995).

Fig. 10 illustrates the triplet structure when the it is well resolved. The figure also shows that this line is very near an order gap in the spectral coverage. This gap produces obvious distortions of the flux. Because of this, we have been unable to determine whether this line could be better fitted by a stratification model. We have arbitrarily raised the observed continuum to fit the calculations at the violet limit of coverage. We also tried *not* applying such a correction, and using various stratification models, but these did not produce improved fits. Better observations are needed to resolve this question. Stratification was not assumed for either plot (Figs 9 and 10) for HD 47103.

We find no evidence – outside of our stated errors – that the measured stellar wavelengths have been affected by proximity to order gaps.

The optimum fits to the λ8498 and λ8662 lines in Figs 9 and 10 used slightly different longitudinal to transverse ratios. It is unclear whether these differences arise from the approximate nature of our Zeeman calculation, or another cause, such as a partial Paschen–Bach effect (Mathys 1990).

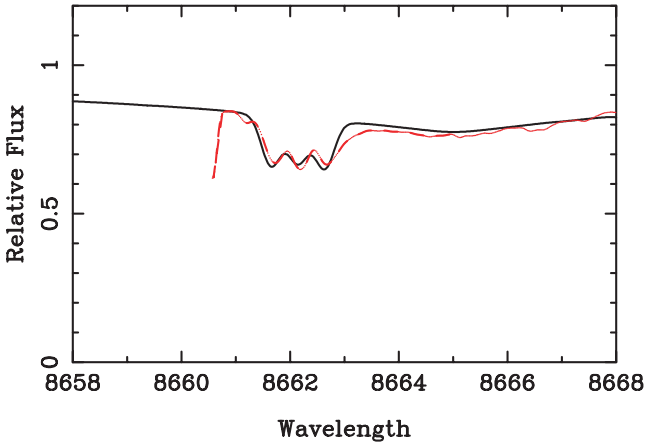

Figure 10. Ca II λ8662 in HD 47103 (17.5 kG). The observational profile on the violet side is unavailable because of an echelle order gap. Optimum fit was obtained with slightly different parameters from those used for the λ8498 line. We used Ca/Sum $= 5.5 \times 10^{-8}$, and a longitudinal to transverse ratio of 1 to 5.

8 SUMMARY

This work is an investigation of the overall interpretation of wavelength shifts in the Ca II spectrum as isotopic. Previous investigations had been based on only two of the three lines of the infrared triplet. Following a reconfiguration of the ESO UVES spectrograph, we were able to measure the third wavelength, λ8542, in 41 additional spectra. The new measurements showed the expected isotopic shifts.

We investigated possible correlations of the isotopic shifts in calcium with temperature, magnetic field strength and isotopic anomalies in mercury. We find a possible *anticorrelation* of isotope shifts with magnetic field strength, perhaps limited to non-oscillating Ap stars. Other correlations, are marginal at best (Section 6).

New measurements of the Hg II λ3984 wavelengths showed that the temperature–isotopic anomaly relation is complicated. It is

extremely puzzling that the Ca-48 anomaly and the Hg-204 (or just heavy Hg) appear uncorrelated. The only current ideas for such anomalies involve chemical fractionation rather than nuclear processes; these ideas would lead us to expect some correlation. The fact that no correlations are yet evident does not vitiate the notion of fractionation, but only means that whatever scenario eventually emerges will be complex.

We found a much weaker overall relation between stellar temperature and the percentage of heavy mercury than previous workers. This is reasonably attributed to our investigation of a wider class of objects – a more diverse group – than was studied in the 1970s (cf. Section 4).

It is too early to conclude that a real, inverse relation exists between the Ca-48 shifts and surface field (see Fig. 6). Perhaps this is fortunate, as at the moment, we can not suggest a reason for the relation.

We synthesized a number of Ca II lines from the infrared triplet in several magnetic stars. In this way we established that valid wavelengths could be obtained even in the presence of considerable Zeeman effects, instrumental perturbations and the proximity of Paschen lines.

Overall fits of the cores and broad wings of λ8498 in γ Equ and λ8542 in HD 51684 required models including stratification for two of our stars. Previous studies have revealed the need for such models. These profile anomalies must be considered along with those for the Balmer lines, and Ca II H and K cores. They clearly indicate differences in the high atmospheric structure of magnetic and normal stars. Since our principal concern in the present paper is with the isotopic wavelength shifts, we leave details of stratified models to the references cited and future work.

ACKNOWLEDGMENTS

We thank Dr G. A. Wade for providing calculations made with a full Stokes transfer that we could use to test our Zeeman procedure. We acknowledge a useful conversation with Dr J. D. Landstreet. This research has made use of the SIMBAD data base, operated at CDS, Strasbourg, France. We appreciate the advice from Dr Jeffrey Fuhr of NIST on oscillator strengths for the Ca II infrared triplet. We acknowledge use of the Vienna Atomic Database (Kupka et al. 1999) and UVES Paranal Observatory Project (ESO DDT Program ID266.D-5655, Bagnulo et al. 2003).

REFERENCES

Babel J., North P., Queloz D., 1995, A&A, 303, L5
Bagnulo S., Jehin E., Ledoux C., Cabanac R., Melo C., Gilmozzi R., The ESO Paranal Science Operations Team, 2003, ESO Mess., 114, 10
Bidelman W. P., 1962, AJ, 67, 111
Bonifacio P., Castelli F., Hack M., 2001, A&AS, 110, 441
Bord D. J., Cowley C. R., Hubrig S., Mathys G., 2003, BAAS, 35, 1357
Castelli F., Hubrig S., 2004, A&A, 421, L1
Castelli F., Hubrig S., 2006, http://wwwuser.oat.ts.it/castelli/hr6000/hr6000.html
Castelli F., Kurucz R. L., 2003, IAU Symp., 210, 20P
Castelli F., Parthasarathy M., Hack M., 1997, A&A, 321, 254
Chmielewski Y., 2000, A&A, 353, 666
Clayton D., 2003, Handbook of Isotopes in the Cosmos. Cambridge Univ. Press, Cambridge, p. 196
Cowley C. R., Aikman G. C. L., 1975, PASP, 87, 513
Cowley C. R., Hubrig S., 2005, A&A, 432, L21
Cowley C. R., Hubrig S., González J. F., Nuñez N., 2006, A&A, 455, L21
del Toro Iniesta J. C., 2003, Introduction to Spectropolarimetry, Cambridge Univ. Press, Cambridge, cf. sections 7.8 and 9.4.2
Dworetsky M. M., 1976, in Weiss W. W., Jenkner H., Wood H. J., eds, IAU Colloq., 32, 553
Federer C. A., 1962, Sky Telesc., 23, 140
Frémat Y., Houziaux L., Andrillat Y., 1996, MNRAS, 279, 25
Hubrig S., North P., Mathys G., 2000, ApJ, 539, 352
Hubrig S. et al., 2005, A&A, 440, L37
Hubrig S., North P., Schöller M., Mathys G., 2006, Astron. Nachr., 327, 289
Kochukhov O., 2007, pre print (astro-ph/0701084)
Kochukhov O., Tsymbal V., Ryabchikova T., Makaganyk V., Bagnulo S., 2006, A&A, 460, 831
Kupka F., Piskunov, N. E., Ryabchikova T. A., Stempels H. C., Weiss W. W., 1999, A&AS, 138, 119
Kurtz D. W., Elkin V. G., Cuhna M. S., Mathys G., Hubrig S., Wolff B., Savanov I., 2006, MNRAS, 372, 286
Lemke M., 1997, A&AS, 122, 285
Mårtensson-Pendrill A.-M. et al., 1992, Phys. Rev. A, 45, 4675
Mashonkina L., Korn A. J., Przybilla N., 2007, A&A, 461, 261
Mathys G., 1990, A&A, 232, 151
Mathys G., Hubrig S., Landstreet J. D., Lanz T., Manfroid J., 1997, A&AS, 123, 353
Moon T. T., 1984, Commun. Univ. London Obs., 78
Muthsam H., Cowley C. R., 1984, ApJ, 130, 348
Nörtershäuser W., Blaum K., Icker P., Muller A., Schmitt A., Wendt K., Wiche B., 1998, Eur. Phys. J. D, 2, 33
Preston G. W., Vaughan A. H., White R. E., Swings J.-P., 1971, PASP, 83, 607
Ryabchikova T. A., 2005a, Pis'ma Astron. Zh., 31, 437 (see also CDS, VIZIE-R J/PAZh/31/437)
Ryabchikova T., 2005b, in Alecian G., Richard O., Vauclair S., eds, EAS Pub. Ser. 17, Element stratificarion in stars: 40 years of Atomic Diffusion. EDP Sciences, Les Ulis, p. 253
Ryabchikova T. A., Adelman S. J., Weiss W. W., Kuschnig R., 1997, A&A, 322, 234
Ryabchikova T., Piskunov N., Kochukhov O., Tsymbal V., Mittermayer P., Weiss W. W., 2002, A&A, 384, 545
Sansonetti J. E., Martin W. F., 2003, Handbook of Basic Atomic Spectroscopic Data, http://physics.nist.gov/PhysRefData/Handbook/index.html
Stehlé C., Hutcheon R., 1999, A&AS, 140, 93
Sugar J., Corliss C. H., 1985, J. Phys. Chem. Ref. Data, 14, 74
Vidal C. R., Cooper J., Smith E. W., 1973, ApJS, 25, 37
White R. E., Vaughan A. H. Jr, Preston G. W., Swings J. P., 1976, ApJ, 204, 131
Woolf V. M., Lambert D. L., 1999, ApJ, 521, 414

APPENDIX A: WAVELENGTH MEASUREMENTS OF CA II INFRARED TRIPLET

Table A1 lists the program stars and the measured Ca II wavelengths.

The λ8542 line was unavailable for many of the stars before reconfiguration of the UVES spectrograph (Section 2). FEROS spectra sometimes included the λ8542 line.

The stars are listed in order of their HD numbers within three categories, mercury–manganese and related stars, traditional magnetic Ap stars and miscellaneous types. The traditional magnetic Ap stars as used here have strong iron-group and lanthanide spectra. Clearly some assignments are arguable, for example, HR 6870 to miscellaneous, and HD 101065 to the traditional category. Oscillating (roAp) and non-oscillating (noAp) stars are indicated.

Entries for HgMn stars and miscellaneous types with the remark 'CH04' are from work of Castelli & Hubrig (2004). Previously unpublished measures on FEROS spectra are labelled 'new'. Entries for magnetic stars and miscellaneous type stars with the remark 'CH05' are from work by Cowley & Hubrig (2005).

Table A1. Stellar wavelength measurements.

HD	Other designation	Spectral type and binarity	NIST wavelengths 8498.02	8542.09	8662.14	Instrument	Remarks
			Mercury–manganese and related stars				
1909	HR 89	B9IV, SB2	0.11		0.14	UVES old	CH04
1909	HR 89		0.14		0.14	FEROS new	
11753	ϕ Phe	B9, SB1	0.15	0.13	0.11	UVES new	
27376	HR 1347 (−)	B9, SB2	0.09	0.10	0.13	UVES new	
27376	HR 1347 (+)		0.16	0.17	0.16	UVES new	
32964	66 Eri A	B9V	0.01	0.05	−0.04	UVES new	
32964	66 Eri B	B9V	0.10	0.13	0.13	UVES new	
33904	μ Lep	B9IV	0.08	0.08	0.08	UVES new	
34364	AR Aur(−)	B9V, SB2	−0.09	−0.03	0.17	UVES new	bad profiles
34364	AR Aur(−)		−0.04	−0.03	0.05	UVES new	diff expos
34364	AR Aur(+)		0.05	0.06	0.03	UVES new	
34364	AR Aur(+)		0.11	0.05	0.02	UVES new	
35548	HR 1800	B9, SB2	0.17	0.17	0.18	UVES new	
65949	CD −60 1951	B8/B9	0.12		0.08	FEROS new	
65949	CD −60 1951	B8/B9	0.12		0.07	FEROS new	
65950	CD −60 1952	B8III	0.15	0.15	0.15	FEROS new	
101189	HR 4487	B9IV	0.09	−0.06	0.06	FEROS old	CH04
124740	CD −40 8541		0.00	0.00	0.00	UVES new	asym to red
141556	χ Lup	B9, SB2	0.00	0.00	0.00	UVES new	asym to red
144667	HR 6000		0.14	0.14	0.14	UVES new	
149121	28 Her	B9, SB1	0.11	−0.04	0.04	FEROS old	CH04
158704	HR 6520	B9, SB2	0.17	0.10	0.19	FEROS old	CH04
165493	HR 6759	B8, SB1	0.20	0.05	0.05	FEROS old	CH04
175640	HR 7143	B9III	0.20	0.20	0.20	UVES old + FEROS old	CH04
178065	HR 7245	B9, SB1	0.16	0.16	0.17	UVES new	
186122	46 Aql	B9III	0.12	0.12	0.12	UVES new	
216494	74 Aqr A	B8 IV/V, SB2	0.03	0.06	0.06	UVES new	
216494	74 Aqr B	B8	0.00	0.01	0.00	UVES new	
221507	HR 3987	B9.5 IV	0.11		0.11	UVES old	CH04
Feige 86	BD +30 2431	HZB star	0.12	0.12	0.12	UVES new	
			Typical magnetic Ap or CP2 stars				
965	BD −00 21	noAp	0.02		0.10	UVES old	CH05
965		noAp	0.02	0.07	0.08	UVES new	
2453	BD +31 59	noAp	0.09	0.10	0.10	UVES new	
15144	HR 710	noAp	0.08	0.11	0.09	UVES new	
24712	HR 1217	roAp	0.15		0.17	UVES old	CH05
47103	BD +20 1508	noAp	−0.02		0.04	UVES old	CH05
50169	BD −01 1414	noAp	0.01		0.07	UVES old	CH05
51684	CD −40 2796	noAp	0.10	0.10	0.11	UVES new	
52696	BD −19 1651	noAp	0.11	0.08	0.08	UVES new	
60435	CD −57 1762	roA	0.06		0.11	UVES old	CH05
75445	CD −38 4907	noAp	0.10		0.17	UVES old	CH05
93507	CD −67 955	noAp	0.01		0.00	UVES old	CH05
94660	HR 4263	noAp	−0.04		0.00	UVES old	CH05
94660			−0.04	−0.05	−0.01	UVES new	
101065	Przybylski's	roAp	0.16		0.18	FEROS old	CH05
101065		roAp	0.19		0.19	UVES old	CH05
116114	BD −17 3829	roAp	0.04		0.02	UVES old	CH05
122970	BD +06 2827	roAp	0.13		0.19	UVES old	CH05
125248	CS Vir	noAp	0.06		0.10	UVES old	CH05, poor
128898	α Cir	roAp	−0.02		0.03	FEROS old	CH04
133792	HR 5623	noAp	0.18		0.18	UVES old	CH05
134214	BD −13 4081	roAp	0.16		0.20	UVES old	CH05
137909	β CrB	roAp	0.10		0.06	UVES old	CH05
137949	33 Lib	roAp	0.00		0.09	UVES old	CH05
176232	10 Aql	roAp	0.14		0.22	UVES old	CH05
187474	HR 7552	noAp	0.02		0.08	UVES old	CH05
188041	HR 7575	noAp	0.04		0.08	UVES old	CH05

Table A1 – *continued*

HD	Other designation	Spectral type and binarity	NIST wavelengths 8498.02	8542.09	8662.14	Instrument	Remarks
201601	γ Equ	roAp	0.08		0.16	UVES old	CH05
201601		roAp	0.09	0.13	0.17	UVES new	First file
201601		roAp	0.08	0.14	0.16	UVES new	Second file
216018	BD −12 6357	noAp	−0.01		0.02	UVES old	CH05
217522	CD −45 14901	roAp	0.18		0.21	UVES old	CH05
			Miscellaneous types				
739	θ Scl	F4 V	0.05		0.05	UVES old	CH05
27411	HR 1353	A3m	0.02		0.08	UVES old	CH05
28187	CD −35 1710	G3 IV/V	0.04	0.04	0.05	UVES new	
84461	o Vel	A0 IV	0.00		0.00	UVES old	CH04
85503	μ Leo	K2 III	0.05		0.06	UVES new	
91375	HR 4138	A1 V	0.00	0.00	0.00	UVES new	
91793	U Ant	N	0.03		0.00	UVES old	CH05
104978	o Vir	G8 III Ba II	0.06		0.07	UVES new	
124897	Arcturus	K1.5 III	0.00		0.00	UVES old	CH05
142860	γ Ser	F6 IV/V	0.03		0.02	UVES new	
146836	HR 6077	F6 III	0.04		0.05	UVES old	CH05
168733	HR 6870	peculiar	−0.05	−0.03	0.03	UVES new	
168733	HR 6870	peculiar	−0.03	−0.02	0.01	UVES new	remeasure
188136	CD −79 790	Fm δ Del	0.02		0.05	UVES new	
193432	ν Cap	B9	0.02	0.02	0.02	UVES new	
196426	HR7878	B9.5 V	0.06	−0.1	0.03	FEROS old	CH04
209459	21 Peg	B8 III	0.02	0.03	0.04	UVES new	
210027	ι Peg	F5 V	0.01	0.03	0.03	UVES new	
214994	o Peg	A1IV	0.03	0.03	0.04	UVES new	

A few notes on individual cases follow.

HD 1909 (HR 89): Rather broad lines. Measurements are for the primary in both entries. Lines from the secondary are difficult to pick out.

HD 32964 (66 Eri): The measurements are for primary and secondary.

HD 34364 (AR Aur): Measurements for violet(−) and red(+) systems of the SB2 were made on different spectra. The profiles belonging to the violet system were of poor quality.

HD 60435: Spectra of this star were of poor quality.

HD 65949: The two entries are from the same FEROS spectrum made on different days.

HD 93507: The λ8662 profile was poor.

HD 124740 and HD 141556 (χ Lup): The minima of all three profiles for primaries (A) of both stars show no shift, but all three profiles have shallow slopes on the red side, indicative of blending. This cannot be Ca II of the secondary, because those lines lie to the violet.

HD 168733: The same UVES spectrum was measured on two different days.

HD 201601 (γ Equ): Measurements on three different exposures are presented.

This paper has been typeset from a TEX/LATEX file prepared by the author.